Biointerphases (2012) 7:64
DOI 10.1007/s13758-012-0064-4

ARTICLE

Layer-by-Layer Assembled Films Composed of "Charge Matched" and "Length Matched" Polysaccharides: Self-Patterning and Unexpected Effects of the Degree of Polymerization

Maria A. Witt · Francine Valenga · Rebecca Blell · Marta E. R. Dotto · Ivan H. Bechtold · Olivier Felix · Alfredo T. N. Pires · Gero Decher

Received: 6 June 2012 / Accepted: 4 October 2012 / Published online: 30 October 2012

Abstract The functionalization of chitosan with carboxymethyl groups allows zwitterionic or anionic chitosan derivatives to be obtained as a function of the degree of substitution. Here, we show that polyelectrolyte multilayers of chitosan and carboxymethylchitosan can be assembled by "dipping" or "spraying" to form strongly hydrated films in which both the polyanion and polycation possess the same polymer backbone ("matched chemistries"). Such films grow rapidly to fairly large thickness in very few assembly steps, especially in the case of "matched" charge densities, and atomic force microscopy reveals the formation of surface patterns that are dependent on the deposition conditions and on the number of layers. Interestingly, the influence of the molar masses of the polyelectrolyte pairs on the complex formation is somewhat counterintuitive, the stronger complexation occurring between polyanions and polycations of different ("non-matching") lengths.

1 Introduction

The development of new materials, particularly composite materials, has increasingly focused on engineering techniques at the nanoscale, both with respect to fundamental science and to potential applications. This is especially true for the field of materials with biological or pharmaceutical applications in which processes such as cell adhesion and tissue growth, gene transfection or drug delivery require control of complex dynamics and transport kinetics [1–4].

A particularly successful method for the functionalization of surfaces and the preparation of nanoscale hybrid films is the layer-by-layer (LbL) assembly technique developed by Decher and co-workers in the 1990s [5, 6]. The versatility of this approach arises from an unprecedented choice of components that can be assembled on almost any solvent-accessible interface. In addition, it offers ease of application, even on large surfaces, nanoscale precision and very good reproducibility. LbL-assembly is usually performed in aqueous media and typically involves the consecutively alternating adsorption of oppositely charged molecules, such as polyelectrolytes or objects such as nanoparticles. In the case of electrostatic interaction it is thought that the adsorption of each layer leads to an overcompensation of the surface charge accompanied by the corresponding counterion release, thus

---

Electronic supplementary material The online version of this article (doi:10.1007/s13758-012-0064-4) contains supplementary material, which is available to authorized users.

M. A. Witt · F. Valenga · R. Blell · O. Felix · G. Decher (✉)
CNRS Institut Charles Sadron, 23 rue du Loess,
67034 Strasbourg, France
e-mail: decher@unistra.fr

M. A. Witt · A. T. N. Pires
Department of Chemistry, Federal University of Santa Catarina,
Florianópolis 88040-900, Brazil

F. Valenga
Department of Biochemistry and Molecular Biology,
Federal University of Paraná, Curitiba 81531-980, Brazil

M. E. R. Dotto · I. H. Bechtold
Department of Physics, Federal University of Santa Catarina,
Florianópolis 88040-970, Brazil

G. Decher
Faculté de Chimie, Université de Strasbourg, 1 rue Blaise Pascal,
67008 Strasbourg, France

G. Decher
International Center for Frontier Research in Chemistry,
8 allée Gaspard Monge, 67083 Strasbourg, France

suggesting predominantly entropic contributions as the driving force for the multilayer build-up.

Nowadays, it can be considered routine to incorporate biological [7], metallic [8] or oxidic nanoparticles [9], nanoplatelets [10, 11], DNA [12], therapeutic compounds [13–15], carbon nanotubes [16], among other components, either individually or as a mixture of different materials, into LbL-assembled films.

For biological or pharmaceutical applications the use of natural polymers is often preferred over synthetic ones for reasons of biocompatibility, bioinertness or biodegradability. Chitosan (CS) is a linear polysaccharide composed of randomly distributed D-glucosamine and *N*-acetyl-D-glucosamine units, which is used in a number of commercial and biomedical applications, prompting also numerous studies in which chitosan was used as a component of LbL-assembled films. In fact the existing literature comprises over 400 articles in this field (see for example Oh et al. [17], Shen et al. [18], Donath et al. [19], Tabrizian et al. [20], Chen et al. [21], Neoh et al. [22], Akashi et al. [23], Voigt et al. [24]). A small drawback of using chitosan, however, lies in its limited solubility, in aqueous solutions with pH values above 6. In consequence, there are many chemical modification of the chitosan backbone through polymer-analog reactions giving rise to better solubilities while maintaining the biological properties of interest. In addition, such reactions allow to even introduce opposite charges, which, depending on the degree of substitution, yields anionic chitosan derivatives. Carboxymethylchitosan (CMCS) is one of the derivatives with enhanced aqueous solubility that are easily obtained. This chemical substitution occurs mainly at the carbons C-2 and C-6 of the glucose unit, but also at C-3, depending on the experimental conditions [25]. What is especially interesting about the use of CMCS for LbL-assembly is the fact that the carboxymethylation reaction leads to the formation of local zwitterions and even to anionic chitosan at high degrees of substitution.

Beside its potential for the preparation of biomaterials with reduced cytotoxicity (polycations are often more cytotoxic than polyanions), the combination of a cationic chitosan derivative with anionic chitosan for LbL-assembly makes it possible to prepare thin films from a single polysaccharide source in which the polyanion and polycation possess the same polysaccharide backbone with close to identical molar masses.

Polyelectrolyte multilayers (PEMs) belong to a class of materials called "Polyelectrolyte Complexes" (PECs), whose investigation became very popular already in the 1950s and the whole field was reviewed numerous times since then (e.g. Tschuchida et al. [26], Bekturov et al. [27], Philipp et al. [28], Kabanov [29], Thünemann et al. [30], Gucht et al. [31]). In general polyelectrolyte complexation is governed by, the charge density along the polymer backbone and thus the pH value in the case of weak polyelectrolytes, the degree of polymerization, the ionic strength as well as the charge balance and difference of the contour lengths of the polyanion/polycation pair and of course temperature. Secondary effects include the chemical nature of the polyelectrolyte main chain and thus persistence length or non-electrostatic interactions such as hydrogen bonding or hydrophobic effects. Strong interpolyelectrolyte interactions (strong polyelectrolytes, long chains, high charge densities, matched chain lengths, stoichiometric composition) lead to more solid-like complexes that precipitate from solution whereas weaker interactions between the polyelectrolytes (weak polyelectrolytes, short chains, low charge densities, asymmetric chain lengths, non-stoiciometric composition) lead to more liquid like complexes that are strongly hydrated and that often stay in solution. A particularly important correlation between classic polyelectrolyte complexation in bulk and "stepwise" polyelectrolyte complexation in LbL-films is believed to be responsible for the growth characteristics of PEMs ranging from regularly growing films (often termed "linear growth") to superlinearly growing films (often termed "exponential growth"). The latter growth type was first described by Schaaf and Voegel [32, 33], the pH dependent matrix for exponentially growing films was investigated by Rubner [34], pH amplified growth was reported by Grunze [35], more recently Schönhoff [36] and Sukhishvili [37] discussed the growth characteristics of PEMs in a more general way.

In view of the numerous parameters that drive polyelectrolyte complexation and the effects of secondary interations it is highly desirable to work with structurally similar polyelectrolytes (see for example Schlenoff [38]) and to keep elementary polymer characteristics as close as possible.

The use of relatively short CMCS chains with long and short CS chains allows the comparison of structurally similar polyanion/polycation pairs with similar and dissimilar contour lengths. It is also desirable to work at a pH value at which both polyelectrolytes are dissociated to the same extent. A weakness of using CMCS in combination with CS is that CMCS is not strictly a polyanion, but an anionic polyzwitterion.

While the effects of for example molar mass, pH or ionic strength have already been investigated in LbL-films in which the cationic component was chitosan (see for example Lvov et al. [39], Berth et al. [40], Picart et al. [41, 42], Winnik et al. [43, 44], Kipper et al. [45], Bomblerg et al. [46]), there is, to the best of our knowledge, no study reporting on LbL-films in which the anionic component of chitosan containing multilayers is also a chitosan derivative and in which the effects of balanced molar mass and balanced charge density were investigated.

Furthermore, such an LbL-film could be considered as a "green" device, being based on natural chitosan and a semi-synthetic derivative of the same polysaccharide.

2 Materials and Methods

2.1 Polyelectrolytes and Chemicals

Poly(ethylene imine) (PEI) ($\overline{M_w} = 25{,}000$ g/mol) and chitosan samples of low molecular weight (CS LMW, $\overline{M_w} \approx 33{,}000$ g/mol) and medium molecular weight (CS MMW, $\overline{M_w} \approx 115{,}000$ g/mol), both with a deacetylation degree of around 80 % (82 and 79 %, respectively, determined previously through ^{1}H-NMR) were used as the polycation. These polymers and the sodium chloride (NaCl) were purchased from Sigma-Aldrich and used without further purification. The CMCS derivative ($\overline{M_w} \approx 20{,}000$ g/mol) was obtained by chemical modification of chitosan (medium molecular weight) with monochloroacetic acid as previously described [25] and used as the polyanion. The average degree of substitution (DS) found for the CMCS through potentiometric titration using a second-order differential method is about 0.5 [47, 48] (note that one sugar unit may carry several carboxymethyl groups). At this degree of substitution the isoelectric point of CMCS is at a pH of about 4 as revealed by zeta potential titration, whereas the unmodified CS has an isoelectric point of about 8.5 clearly confirming that CS is a polycation and that CMCS is a polyanion. All polyelectrolyte solutions were prepared using Milli-Q water. The concentration of the PEI solution was 2.5 mg/mL and for all the other polyelectrolyte solutions it was 1.0 mg/mL containing 0.15 mol/L of NaCl. The pH values of the CS and CMCS polyion solutions were adjusted to 6.0 and 6.5, respectively, by the addition of appropriate volumes of either NaOH solution or HCl solution prior to the LbL deposition. We would have preferred to work at a pH value of 6.25 for both polyelectrolyte solutions which corresponds to the pH value at which both polyions are dissociated to the same extent, but unfortunately both CS and CMCS start to precipitate at pH 6.25.

2.2 LbL-Assembly

Silicon wafers with an orientation of 100 and a thickness of 0.5 mm were purchased from WaferNet, Inc. (San Jose, USA) and used as substrates. They were cleaned prior to the polyelectrolyte deposition by rinsing with ethanol (analytical grade) and then treated with plasma (Harrick Plasma, Ithaca, NY) for 3 min at medium power. The multilayer assembly was performed either by dipping or via a spray-assisted assembly procedure. For the LbL-assembly by dipping the charged substrates were firstly immersed in PEI solution for 10 min. They were rinsed twice with ultrapure (Milli-Q) water for 5 min and each time the surface was primed with a positive charge. The substrates were then dipped alternately in polyanion (CMCS) and polycation (CS) solutions for 15 min. They were rinsed twice with ultrapure water (5 min) after the deposition of each layer. This cyclic procedure was repeated until the final number of layer pairs was deposited. For the spray-assisted LbL-assembly AirBoy Spray cans (Carl Roth GmbH&Co.) were used to spray the respective solution for 5 s onto the substrate, followed by 5 s of spray-rinsing with ultrapure water. After each step, the solution was allowed to drain for 10 s prior to the next spraying step. After every rinsing step (Milli-Q water) the film was dried using a stream of compressed air and characterized by ellipsometry or atomic force microscopy (see below).

2.3 Ellipsometry

The thickness of the assembled multilayers on the silicon wafer substrate was measured in the dry state with a PLASMOS SD 2300 ellipsometer at a wavelength of 632.8 nm and an angle of incidence of 70°. The refractive index of the polyelectrolyte film was assumed to be constant ($n = 1.465$). While this procedure gives slightly incorrect values with respect to the absolute film thickness, it allows for the quick and precise determination of the relative film thickness. The thickness of each layer (each data point on the graph) is calculated as the average of the measurements randomly taken at different points on the film surface. All measurements were carried out at ambient temperature and humidity.

2.4 Atomic Force Microscopy (AFM)

The samples for the AFM measurements were prepared by classic dipping described above with a film architecture Si/PEI/(CMCS/CS)$_n$ where $n = 2, 5, 10$ or 20 for films terminating with a layer of CS and $n = 2.5, 5.5, 10.5$ or 20.5 for films terminating with a layer of CMCS. The topographical images were collected using a NanoSurf® easyScan 2 AFM microscope in the tapping mode applying a scanning rate of 1.0 Hz, using silicon nitride cantilevers with a resonance frequency of 190 kHz, force constant of 48 N/m and image resolution of 512 × 512 pixels. All measurements were carried out at ambient temperature and humidity.

2.5 Quartz Crystal Microbalance (QCM-D)

The multilayer deposition was monitored in situ using a Quartz Crystal Microbalance QCM-D (Q-Sense, Göteborg, Sweden). This technique consists of measuring the changes in the resonance frequency (Δf) upon adsorption of the chemical species in solution. Data were collected at the fundamental frequency (5 MHz) and up to the fifth overtone. For thin and rigid films the change in resonance frequency (Δf) is converted to the adsorbed mass (Δm) using the Sauerbrey equation [49].

$$\Delta m = -C \times \left(\frac{\Delta f}{v}\right) \qquad (1)$$

where ν is the overtone number and C the mass sensitivity constant (for the QCM-D system C ≈ 17.7 ng/cm^{-2} Hz at $f = 5$ MHz in air).

This adsorbing surface (gold electrode) was cleaned prior to use by extensive rinsing with ethanol (analytical grade) and then treated with plasma (Harrick Plasma, Ithaca, NY) for 3 min at medium power. For each run the gold surface was primed with a polycation layer by injecting 700 µL of PEI solution, and then rinsed twice with the same volume of pure water. The injection of the solution for the adsorption of the next layer was carried out only after the stabilization of the frequency and dissipation signals. For the polyelectrolyte multilayer assembly 700 µL of a 0.15 mol/L NaCl solution was used as the rinsing solution. Subsequently, similar volumes of CMCS and CS solution where injected, followed by two rinsing steps with 0.15 mol/L NaCl solution.

3 Results

3.1 Ellipsometric Thicknesses of Different $(CMCS/CS)_n$ Multilayers: Effects of pH and Molar Mass

Once this polyelectrolyte pair (Fig. 1) is formed for both species considered as weak polyelectrolytes, the dissociation behavior and consequently the total charge density along the chain varies as the pH of the medium changes. Some previous studies have demonstrated the influence of pH on the multilayer build up, presenting distinct regimes of growth when this class of polymer (weak polyelectrolytes) is used [36]. The chemical modification of the CS MMW to obtain the CMCS derivative caused a reduction in the molar mass from around 115,000 g/mol to around 20,000 g/mol, estimated applying the viscosimetric method as described by Zhai et al. [50]. This method involves the use of an Ostwald capillary viscosimeter [a complete description of the procedure used to estimate the CMCS molecular weight is given in the Electronic Supplementary Information (ESM)].

Figure 2 shows that it is impossible to assemble multilayer films from this combination of polyelectrolytes when they are used at the initial pH values of the corresponding solutions (pH = 3.5 for CS and pH = 8.15 for CMCS).

Zeta potential titration revealed that CMCS has an isoelectric point at a pH of about 4, whereas the unmodified CS has an isoelectric point of about 8.5. We would have preferred to work at a pH value of 6.25 for both polyelectrolyte solutions which corresponds to the pH value at which both polyions are dissociated to the same extent, but unfortunately both CS and CMCS start to precipitate at pH 6.25. Thus the pH values of the CS and CMCS polyion solutions were adjusted to 6.0 and 6.5, respectively, by the addition of appropriate volumes of either NaOH solution or HCl solution prior to the LbL deposition. The pH of the deposition solutions plays a very important role in polyelectrolyte complex formation and also in multilayer deposition for example observed with the the “soft” polyelectrolyte pair poly(acrylic acid)/poly(allyl amine hydrochloride) (PAA/PAH) [34]. So-called “amplified exponential growth” was observed by choosing asymmetrical pH conditions for the assembly of poly(acrylic acid)/poly(ethylene imine) (PAA/PEI), as demonstrated by Grunze et al. [35]. A more general picture of the influence of the pH on polyelectrolyte multilayer formation was presented more recently [36, 37].

While pH values of 6.0 and 6.5 led to a slight but symmetric reduction in the total charge density for both polyelectrolytes (“matched charge densities”), these conditions lead to good multilayer growth (Fig. 2).

In the present study, for a specific number of layer pairs (10 layer pairs—denoted by the vertical dotted line in Fig. 2) the total thickness of the films constructed by the dipping method (Fig. 2a) is higher than that obtained for spray-assembled films (Fig. 2b). This behavior has been observed for several systems [51–53], and may be due to shorter contact times of the liquid with the surface in the case of spraying, due to temperature-induced effects arising from

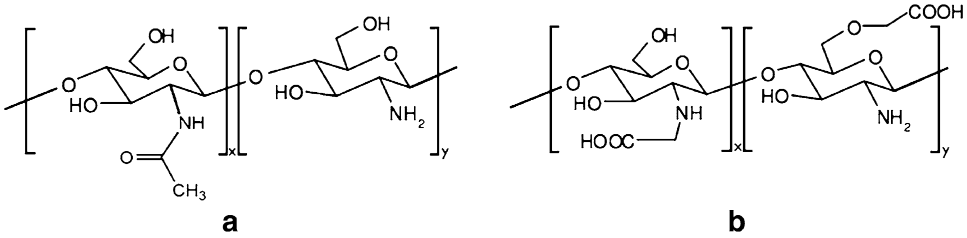

Fig. 1 Chemical structures of the acetylated and deacetylated units of cationic chitosan [CS] (**a**) and *N*-carboxyl and *O*-carboxyl units of anionic carboxymethylchitosan (CMCS) (**b**), respectively

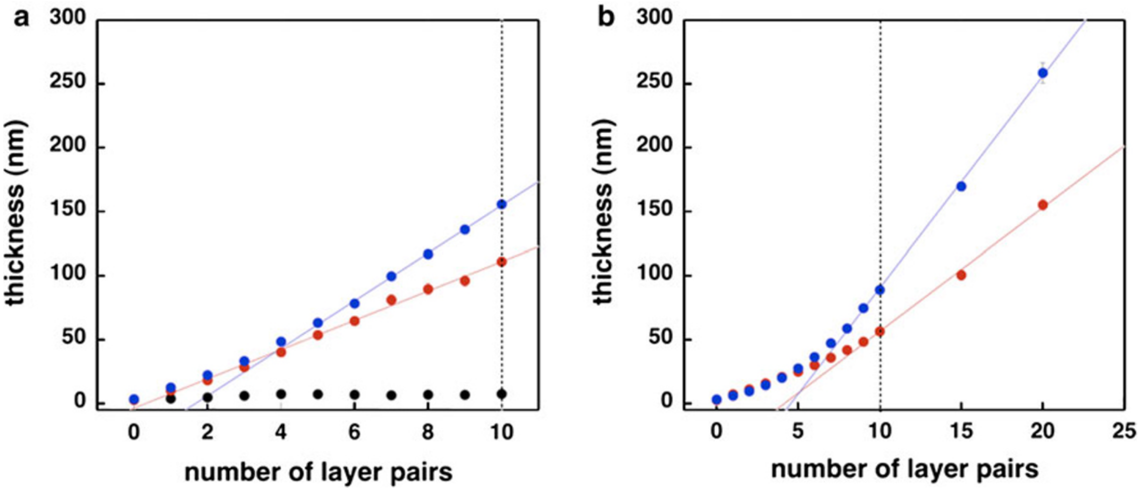

Fig. 2 LbL build up of the system (CMCS/CS)$_n$ as a function of the number of layer pairs deposited by dipping (**a**) and spraying (**b**), measured by ellipsometry. CS LMW (*blue line*) and CS MMW (*red line*) were used for the assembly of (CMCS/CS)$_n$ films. The (CMCS/CS)$_n$ film assembly at initial pH of both polyelectrolyte solutions (*black line*) is indicated only on graph **a**. The slope of the curves at **a** for CS LMW (18.6 nm/per layer pair) and CS MMW (11.5 nm/per layer pair; R = 0.998) and at **b** for CS LMW (16.6 nm/per layer pair; R = 0.999) and CS MMW (9.7 nm/per layer pair; R = 0.998) indicate the thickness per layer pair. Note that the slopes are taken at higher layer numbers after film growth reached a linear regime

the evaporation of spray droplets but may also be due to different spray-induced shearing effects. The thicknesses per layer pair (TI, obtained from the slopes of the growth curves, Fig. 2) were similar for CS LMW (*blue circles*) films deposited by dipping ($\mathrm{TI}_{\mathrm{CSLDIP}} = 18.6$ nm/per layer pair, Fig. 2a) and by spraying ($\mathrm{TI}_{\mathrm{CSLSPRAY}} = 16.6$ nm/per layer pair, Fig. 2b). This finding also applied to the CS MMW (*red circles*) ($\mathrm{TI}_{\mathrm{CSMDIP}} = 11.5$ nm/per layer pair, Fig. 2a and $\mathrm{TI}_{\mathrm{CSMSPRAY}} = 9.7$ nm/per layer pair, Fig. 2b). In all cases, for the same deposition method (dipping or spraying), the films containing CS LMW were thicker than those with CS MMW by a factor of around 1.65. This is interesting because the deacetylation degrees of the two polyelectrolytes were very similar (82 and 79 %). In a previous study Picart et al. [41] reported on the influence of the CS molar mass in the layer thickness for LbL-films composed of higher molar mass chitosans with hyaluronic acid (HA). The results showed that the film buildup was more rapid when the mass of CS (diffusing species) used was smaller.

The possibility of controlling the surface morphology of such LbL-films is of particular interest in relation to the correlation between topology features and the size of the PECs in the bulk material. Recently, the combination of poly(sodium phosphate) and poly(allylamine hydrochloride) (PSP/PAH) resulted in a multilayer assembly with an unusual film-forming behavior concerning the zeta potential and surface morphology as a function of the number of deposited layers [54]. In addition, Ball et al. [55] have demonstrated, through morphological changes, the influence of the chemical nature of the polyelectrolytes on the adsorption kinetics and exchange processes in the film.

3.2 Surface Morphologies of Different (CMCS/CS)$_n$ Multilayers: Effects of pH, Molar Mass and of the Outermost Layer

In Fig. 3a the morphology of the films constructed by dipping as a function of the number of layer pairs (2, 5, 10, and 20) was evaluated for the CS samples of different molecular weights. In general, the formation of multilayer films seems to start as a consecutive deposition of granular structures as the complexation of the polyelectrolytes of opposite charges occurs at the surface.

A uniform surface coverage, as observed by AFM, is achieved after deposition of five layer pairs, regardless of the molecular weight of the CS used. Ellipsometry showed that the growth behaviour of these films can be separated into two parts, the second of which can be treated as linear. The transition to linear growth occurs also after the deposition of about five layer pairs indicating the influence of the underlying substrate becomes negligible at that point and linear growth sets in the case of CS LMW. The transition to linear growth for the higher molecular weight derivative CS MMW occurs a little later at about seven layer pairs.

Figure 3b shows the AFM topologies and line profiles for the (CMCS/CS)$_n$ films which indicate that the granular surface features increase with increasing layer numbers. In addition, the films containing the CS with the higher molar mass (CS MMW, bottom) exhibited slightly larger features than the films containing the CS with the smaller mass (CS LMW, top).

Figure 4a shows the AFM images of the same films but terminating with a layer of CMCS (polyanion). In

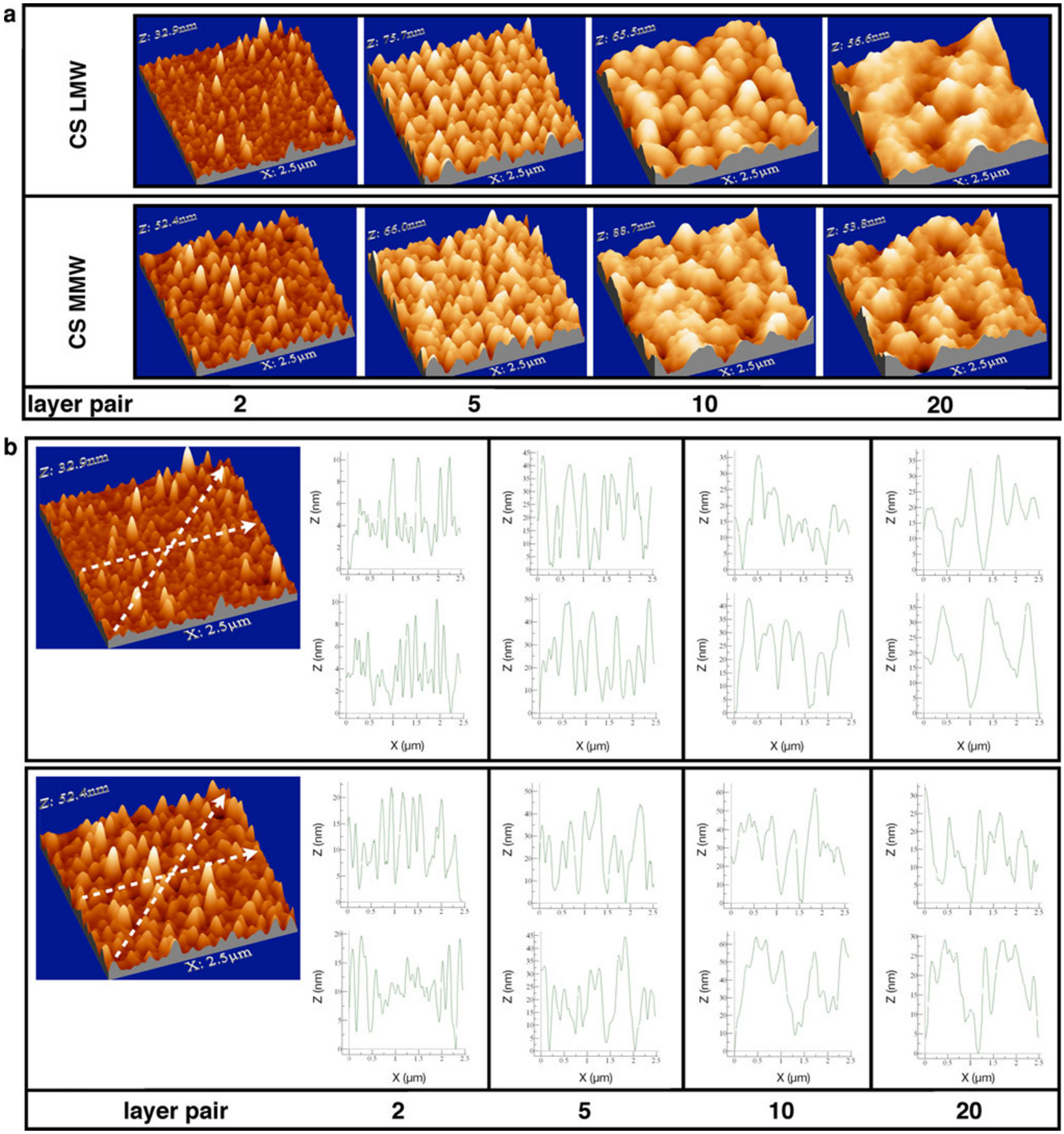

Fig. 3 **a** Surface morphology of the LbL-films composed of 2, 5, 10, and 20 layer pairs of $(CMCS/CS)_n$. The 3D images of the films at the top were obtained with CS of low molecular weight and at the bottom with CS of medium molecular weight. **b** AFM topologies and line profiles of LbL-films composed of 2, 5, 10, and 20 layer pairs of $(CMCS/CS)_n$ composed of CS LMW (*top*) and CS MMW (*bottom*). All films terminate with a layer of CS. The lines along which the profiles were taken are indicated by *white dotted arrows*. The topological images were taken at n = 2 and the evolution of the film topology as a function of n is evidenced by the line scans on the right side of each row. The image dimensions are 2.5 × 2.5 μm^2, and the maximum *Z*-ranges in (**b**) are 20 nm (n = 2), 50 nm (n = 5), 60 nm (n = 10) and 35 nm (n = 20)

principle, the topology differences are small, the most notable being a slightly more pronounced presence of larger features in thicker films terminating with a layer of CS. Films terminating with CMCS show more small aggregates at higher layer numbers, for example, at n = 20.5 (Fig. 4a).

The terminating layer of CMCS does not induce a significant difference for the average surface roughness values [Root Mean Square (RMS)] in relation to the CS molecular weight used for the multilayer assembly, as shown in Table 1.

The films assembled under conditions where the pH of the polyelectrolyte solutions is not pH = 6.0 and pH = 6.5, respectively showed a pronounced self-patterning effect in which the feature size increases with increasing layer numbers (Fig. 4b). Similarly to a LbL-film composed of (PSP/PAH) [54], the films obtained under these conditions could provide a new and interesting case of self-patterning, with the largest feature sizes in the order of 100–150 nm. This control of the surface morphology is unexpected as dynamic surface phenomena (i. e. diffusion of polyelectrolytes) should lead to a decrease in surface roughness with increasing layer numbers due to surface tension, whereas surface patterns in kinetically trapped films are expected to show only slightly changes in their morphology (i. e. growth of features sizes).

Grunze et al. [56] described the antifouling properties of a poly(acrylic acid) and poly(ethylene imine) (PAA/PEI) LbL-film. In this system, the attachment of zoospores of *Ulva* was controlled by the feature size of the morphological structures

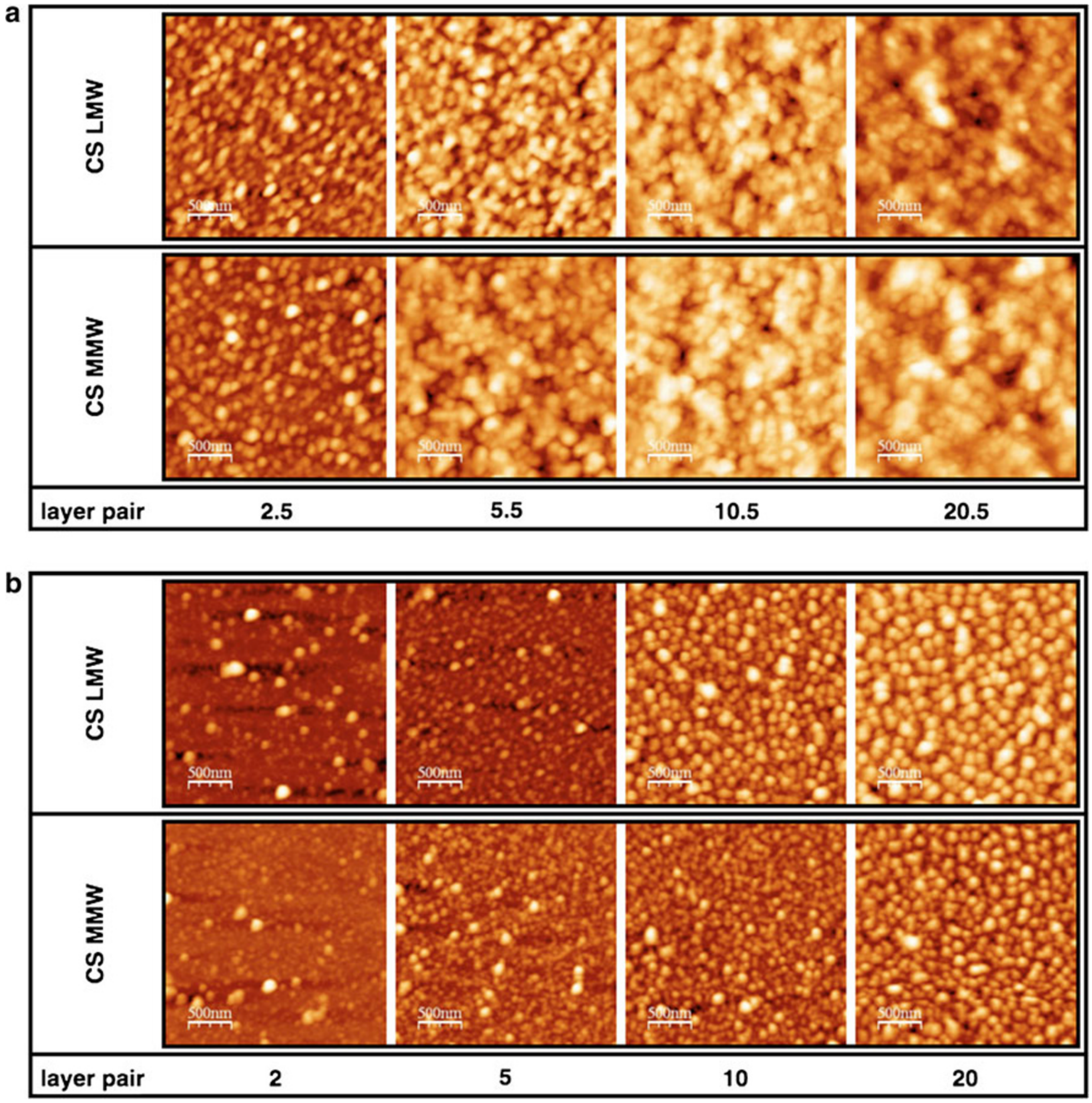

Fig. 4 **a** Surface morphology of the LbL-films of $(CMCS/CS)_n$ composed of 2.5, 5.5, 10.5, and 20.5 layer pairs using chitosan low molecular weight (CS LMW) or medium molecular weight (CS MMW). Note that all n values correspond to an uneven number of layers and so all films terminate with a layer of CMCS. **b** Surface morphology of the LbL-films of $(CMCS/CS)_n$ composed of 2, 5, 10, and 20 layer pairs at the initial pH solution using chitosan of low molecular weight (CS LMW) and medium molecular weight (CS MMW). The image dimensions are 2.5 × 2.5 μm^2

Table 1 RMS values of the LbL-films $(CMCS/CS)_n$ as a function of the layer pairs (LP), with CS LMW, CS MMW, or CMCS as the terminating layer (bold)

System	Roughness RMS (nm)			
	2 LP	5 LP	10 LP	20 LP
(CMCS/**CS LMW**)	3.2	12.0	10.0	8.7
(CMCS/**CS MMW**)	6.5	11.0	14.0	8.5
System	Roughness RMS (nm)			
	2.5 LP	5.5 LP	10.5 LP	20.5 LP
(**CMCS**/CS LMW)	7.6	12.0	16.0	11.0
(**CMCS**/CS MMW)	6.9	11.0	13.0	11.0

All films were prepared under adjusted pH conditions

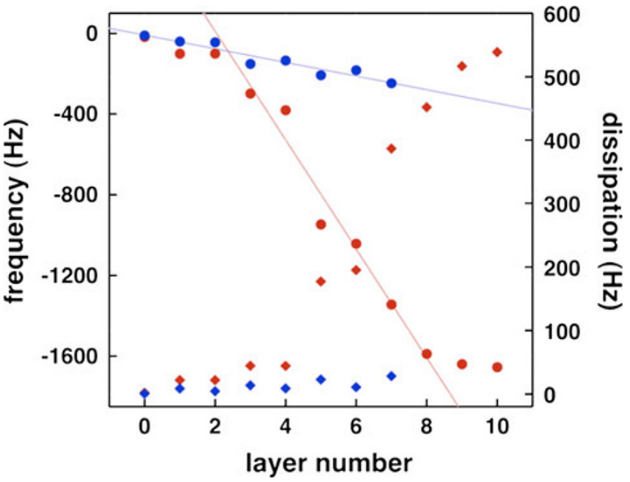

Fig. 5 Frequency change (*filled circles*, *left axis*) and dissipation change (*filled rhombi*, *right axis*) during the LbL deposition of $(CMCS/CS)_n$ using CS of low (*red line*) and medium (*blue line*) molecular weight. The corresponding slope of the curve frequency with CS LMW is −269.5 Hz per layer (R = 0.982) and with CS MMW is 33.9 Hz per layer (R = 0.956). Data are reported for the base resonance frequency (5 MHz)

with the lowest level of settlement occurring for structures with the same order of magnitude as the cell size (≈2 μm).

3.3 Adsorbed Mass and "Stiffness" of Different $(CMCS/CS)_n$ Multilayers as Observed by Quartz Crystal Microbalance (QCM)

The multilayer build up was also monitored in situ by quartz crystal microbalance, the changes in the frequency and dissipation values upon polyelectrolyte adsorption are shown in Fig. 5. The mass increase during layer formation is proportional to the decrease of the resonance frequency (left axis on the graph). Using chitosan with distinct molecular weights, a considerable difference in the amount of polymer adsorbed was observed. The films obtained with CS LMW showed a different behavior with respect to both the amount of polyelectrolyte adsorbed (frequency) and the viscoelastic properties (dissipation) compared to those obtained using CS MMW. Note that the apparent "leveling off" of the frequency shift for CS LMW films with eight layers is very likely an artifact associated with the QCM method. At this film thickness, the mechanical excitation of the film no longer reaches the film surface and thus the newly adsorbing layers are not "seen" by the QCM. The thickness of films prepared using similar dipping times and solution conditions as those applied for the QCM-D was also measured by AFM to demonstrate that the "leveling off" behavior observed in Fig. 5 does not correspond to a discontinuation of film growth but is caused by reaching the experimental limits of the QCM-D instrument. The AFM analysis (see ESM) reveals that the thickness of the films continues to grow beyond the deposition of eight layers, in agreement with ellipsometry data that clearly confirms the continued growth.

Although the Sauerbrey equation (Eq. 1) is only valid for the calculation of the adsorbed mass of rigid films with low dissipation values [49], we used it to estimate the adsorbed mass in the range of 3–8 layers for CS LMW films and for any layer number for CS MMW films. The adsorbed Sauerbrey mass per layer pair was 1,908.2 ng/cm^{-2} for CS LMW (*red symbols*) and 240.0 ng/cm^{-2} for CS MMW (*blue symbols*). These values agree well with the observed dissipation (D) values indicating that films composed of CS LMW (D about 500) contain much more water than films composed of CS MMW (D about 20). This comes somewhat as a surprise, since judging from polyelectrolyte complex formation in bulk, the complex formed by a polyelectrolyte pair with "matched length" would be expected to be less soluble and thus less swollen than a complex formed by polyelectrolytes of unequal length. This is even more surprising, since the both polyanion and polycation are based on the same polysaccharide backbone ("matched chemistries" [38]) and since we are depositing at a pH value at which both polyions have the same degree of dissociation ("charge matching"). At present we have no explanation of this behavior, a plausible reason for the observed deviation could be that the CMCS is not a true polyanion but an anionic polyzwitterion. Another possibility for the observed phenomenon could be that the determination of the pH value at which the "charge matching" occurs is not exact enough due to a systematic lack of precision of the zeta potential measurements.

4 Summary and Conclusions

We report here another case of polyelectrolyte multilayer films in which granular surface features are controlled by the number of layers deposited. The previously described case of this type of self-patterning [54] was observed for films composed of poly(sodium phosphate) and poly(allyl amine). As in this previous case the surface features became larger with increasing film thickness. This is somewhat unexpected since the surface features of films that are prone to change (dynamic PECs) would be expected to lead to smooth films after the deposition of a few layers due to the action of surface tension. This smoothing of surfaces has been previously observed with LbL-films composed of hyaluronic acid and poly(L-lysine) [57], and smooth films have also been observed, for example, with soft polyelectrolytes such as poly(acrylic acid) and poly(allyl amine). The control of the feature size of surface patterns is an interesting new aspect in the field of PEMs because this technique is easily applicable to large surface areas for which patterning is difficult to obtain with low cost methods.

A second interesting unexpected finding concerns the LbL-assembly of chitosan and CMCS as a function of the molar mass of the polycation. In the study reported herein we used low and medium mass chitosan (CS LMW, $\overline{M_w} \approx 33{,}000$ g/mol and CS MMW, $\overline{M_w} \approx 115{,}000$ g/mol) both with a deacetylation degree of 80 % and a low mass CMCS derivative ($\overline{M_w} \approx 20{,}000$ g/mol). In general, chain–chain interactions in PECs are considered to be stronger in the case of comparable charge densities and in the case of similar chain lengths stronger interaction is expected to lead to denser, less hydrated complexes. In the present case the charge densities were matched by depositing from a solution pH of 6.0 and 6.5, respectively for both chitosan chain lengths and thus strong effects from the average charge-to-charge distances along the polyion chains would not be expected.

In this study both ellipsometry and quartz crystal microbalance techniques showed that the polyanion/polycation pair composed of polymers of low mass forms thicker layers than LbL-films composed of polyelectrolytes with asymmetric contour lengths. It is counterintuitive that films composed of two short chains are thicker than films in which one member of the pair has a considerably larger molar mass and this suggests an unusual complex formation in this case. Clearly, the observed differences in film growth could also be due to other effects, for example, to the fact that carboxymethylchitosam is not a true polyelectrolyte but an anionic polyzwitterion.

Nevertheless, the fact that two small and oppositely charged polyelectrolytes with identical polysaccharide backbones can be assembled into highly hydrated multilayer films (interpreting large dissipation values in the QCM-D measurements as a consequence of hydration) which grow rapidly to fairly large thickness in very few assembly steps is promising for biological applications.

Acknowledgments This research was funded by the Coordination for the Improvement of Higher Level Personnel (CAPES/Brazil), National Council of Technological and Scientific Development (CNPq/Brazil—Grant MCT/CNPq 74/2010) and by the Centre National de la Recherche Scientifique (CNRS/France). G. Decher gratefully acknowledges support from the “Institut Universitaire de France”.

References

1. Hammond P (2004) Adv Mater 16:1271–1293
2. Kotov NA, Tang Z, Wang Y, Podsiadlo P (2006) Adv Mater 18:3203–3224
3. Ariga K, Hill JP, Ji Q (2007) Phys Chem Chem Phys 9:2319–2340
4. Caruso F, Becker AL, Johnston APR (2010) Small 6:1836–1852
5. Decher G, Hong JD, Schmidt J (1992) Thin Solid Films 210:831–835
6. Decher G (1997) Science 277:1232–1237
7. Möhwald H, Lvov Y, Haas H, Decher G (1994) Langmuir 10:4232–4236
8. Decher G, Schmitt J, Dressick WJ, Brandon SL, Geer RE, Shashidhar R, Calvert JM (1997) Adv Mater 9:61–65
9. Fendler JH, Kotov NA, Dékány I (1995) J Phys Chem 99: 13065–13069
10. Ferguson GS, Kleinfeld ER (1994) Science 265(5170):370–373
11. Mallouk TE, Kaschak DM (1996) J Am Chem Soc 118: 4222–4223
12. Jessel N, Oulad-Abdelghani M, Meyer F, Lavalle P, Haîkel Y, Schaaf P, Voegel JC (2006) P Natl Acad Sci USA 103:8618–8621
13. Decher G, Schneider GF, Subr V, Ulbrich K (2009) Nano Lett 9:636–642
14. Hammond P, Kim BS, Smith RC, Poon Z (2009) Langmuir 25:14086–14092
15. Srivastava R, Jayant RD, McShane MJ (2011) Int J Pharm 403:268–275
16. Cui T, Lee D (2011) Lagmuir 27:3348–3354
17. Oh JK, Drumright R, Siegwart DJ, Matyjaszewski K (2008) Prog Polym Sci 33:448–477
18. Shen G, Yang M, Yang Y, Yang H, Yu R (2006) Biomaterials 27:246–255
19. Donath E, Qiu X, Leporatti S, Möhwald H (2001) Langmuir 17:5375–5380
20. Tabrizian M, Thierry B, Winnik FM, Merhi Y, Silver J (2003) Biomacromolecules 4:1564–1571
21. Chen Q, Wu BY, Hou SH, Yin F, Li J, Zhao ZX, Huang JD (2007) Biosens Bioelectron 22:838–844
22. Neoh KG, Chua PH, Kang ET, Wang W (2008) Biomaterials 29:1412–1421
23. Akashi M, Serizawa T, Yamaguchi M (2002) Biomacromolecules 3:724–731
24. Voigt A, Lichtenfeld H, Sukhorukov GB, Zastrow H, Donath E, Bäumler H, Möhwald H (1999) Ind Eng Chem Res 38:4037–4043
25. Park HJ, Chen XG (2003) Carbohydr Polym 53:355–359
26. Tsuchida E, Osada Y, Abe K (1973) Makromol Chem 175:583–592

27. Bekturov EA, Bemendina LA (1981) Adv Polym Sci 41:99–147
28. Philipp B, Dautzenberg H, Linow KJ, Kötz J, Dawydoff W (1989) Prog Polym Sci 14:91–172
29. Kabanov VA (1994) Polym Sci 36(2):143–156
30. Thünemann AF, Müller M, Dautzenberg H, Joanny JF, Löwen H (2004) Adv Polym Sci 166:113–171
31. Gucht J, Spruijt E, Lemmers M, Cohen Stuart MA (2011) J Colloid Interface Sci 361:407–422
32. Schaaf P, Voegel JC, Picart C, Lavalle Ph, Hubert P, Cuisinier FJG, Decher G (2001) Langmuir 17:7414–7424
33. Schaaf P, Voegel JC, Picart C, Mutterer J, Richert L, Luo Y, Prestwich GD, Lavalle Ph (2002) P Natl Acad Sci USA 99(20):12531–12535
34. Rubner MF, Shiratori SS (2000) Macromolecules 33:4213–4219
35. Grunze M, Fu JH, Ji J, Shen LY, Kueller A, Rosenhahn A, Shen JC (2009) Langmuir 25:672–675
36. Schönhoff M, Bieker P (2010) Macromolecules 43:5052–5059
37. Sukhishvili S, Xu L, Pristinski D, Zhuk A, Stoddart C, Ankner JF (2012) Macromolecules 45:3892–3901
38. Schlenoff JB, Al-Hariri LA, Reisch A (2011) Langmuir 27:3914–3919
39. Lvov Y, Onda M, Ariga K, Kunitake T (1998) J Biomat Sci—Polym E 9:345–355
40. Berth G, Voigt A, Dautzenberg H, Donath E, Möhwald H (2002) Biomacromolecules 3:579–590
41. Picart C, Richert L, Lavalle P, Payan E, Shu XZ, Prestwich GD, Stoltz JF, Schaaf P, Voegel JC (2004) Langmuir 20:448–458
42. Picart C, Schneider A, Etienne O, Mutterer J, Schaaf P, Egles C, Jessel N, Voegel JC (2005) Adv Funct Mater 15:1771–1780
43. Winnik FM, Kujawa P, Moraille P, Sanchez J, Badia A (2005) J Am Chem Soc 127:9224–9234
44. Winnik FM, Kujawa P, Badia A (2006) J Nanosci Nanotechn 6:1565–1574
45. Kipper MJ, Boddohi S, Killingsworth CE (2008) Biomacromolecules 9:2021–2028
46. Bomblerg E, Lundin M, Solaqa F, Thormann E, Macakova L (2011) Langmuir 27:7537–7548
47. Chen XG, Wang LC, Liu CS, Li PW, Zhou YM (2008) J Polym Sci Polym Phys Ed 46:1419–1429
48. Ge HC, Luo DK (2005) Carbohydr Res 340:1351–1356
49. Sauerbrey GZ (1959) Phys 155:206–222
50. Zhai M, Huang L, Peng J, Li J, Wei G (2007) Carbohydr Polym 67:305–312
51. Schlenoff JB, Dubas ST, Farhat T (2000) Langmuir 16: 9968–9969
52. Decher G, Izquierdo A, Ono SS, Voegel JC, Schaaf P (2005) Langmuir 21:7558–7567
53. Decher G, Felix O, Zheng Z, Cousin F (2009) CR Acad Sci II C 12:225–243
54. Decher G, Cini N, Tulun T, Ball V (2010) J Am Chem Soc 132:8264–8265
55. Ball V, Laachachi A, Toniazzo V, Ruch D (2012) J Colloid Interface Sci 366:96–104
56. Rosenhahn A, Cao X, Pettitt ME, Wode F, Sancet MPA, Fu J, Ji J, Callow ME, Callow JA, Grunze M (2010) Adv Funct Mater 20:1984–1993
57. Picart C, Lavalle P, Hubert P, Cuisinier FJG, Decher G, Schaaf P, Voegel JC (2011) Langmuir 17:7414–7424